An Analytical Solution to Transform O-cell Pile Test Data into Conventional Load-settlement Curve

Xiao-zhou XI[1], Long-zhu CHEN[1], Wei LIU[1,2]

1 Institute of Engineering Safety and Disaster Prevention, Dept. of Civil Engineering, Shanghai Jiao Tong University, Shanghai 200240, China
2 Dept. of Civil Engineering, Ningbo Institute of Technology, Zhejiang University, Ningbo 315100, China

ABSTRACT: In this paper, an analytical method is proposed to transform the results of Osterberg-Cell pile testing (OPT) to conventional load-settlement curve of pile, which is loaded downward at the pile top. First, a tri-linear load transfer function representing pile side resistance was used to analyze the OPT of the pile segment above the Osterberg Cell. Parameters needed for the transfer function were obtained by fitting the OPT data. The self-weight of the upper pile segment was taken into account. As the friction between soil and pile in OPT has opposite direction compared to that of the conventional test, the downward transfer function has been transformed into the upward function. The OPT data of the lower pile segment was considered as boundary conditions of the upper segment of the equivalent top-loaded pile to transform the OPT data into conventional results with the upward friction obtained above. Case histories were used to validate that the conventional pile load-settlement curve obtained using this analytical method compared well with the measured data.

1 INTRODUCTION

Self-Balanced testing method is an up-to-date static pile testing approach. In this method, specially designed loading equipment, viz. Osterberg Cell is placed at the specified location along piles, with hydraulic pipes and displacement transducer wires extended to the ground surface. Hydraulic jack provides hydraulic pressure into the loading cell, which applies loads to the test piles. In this approach, actual loading is in equilibrium with frictions between upper-segment of the pile and the soil, self-weight of pile, frictions of lower-segment of pile and pile tip resistance. The capacity of the pile can be obtained from the two load-displacement curves of the upper and the lower segment of pile. This approach was first introduced into practices by Osterberg (1989) and is referred as Osterberg-Cell load test or O-cell load test. This method has been widely used for its simple instrumentation and lower expense, especially with no needs of reaction piles or massive mass.

Since the mechanism of load transfer and soil-pile interactions in an O-cell load test is similar to that in a conventional static pile test, allowing this method considered as a reliable testing approach. However, the mode of load transfer in a self-balanced load test is different from that in a static load test consequently a certain transform approach is required to convert test data into a pile top load-settlement relationship. Empirical method and displacement harmony method are two kinds of such converting methods (GONG et al., 2002, and JIANG et al., 2006). However, the empirical method lacks sufficient theoretical explanation, and the displacement harmony method requires transmission functions for each layer of soil from field measurements. The load transfer method described herein divides the pile into several elastic elements with nonlinear springs connected in-between to simulate the load transfer mechanism between piles and soil (Seed and Reese, 1957, and CHEN et al., 1995). With static equilibrium and elastic theory, the analytical description about the behavior of piles can be derived, which requires the assumptions about loading transfer functions.

There have been quite number of research works confirmed that the hyperbolic function is suitable to simulate the loading transform. However, it was realized that the hyperbolic function is difficult to be solved and therefore was simplified into multi-linear functions (CHEN et al., 1994). This paper adopts a tri-linear model to simulate the load transfer of piles. In this method, the analytical expression of a load-displacement relationship for the upper-segment of piles is obtained with consideration of the pile self-weight. With comparisons with actual measurement, the parameters of load transfer function can be obtained. Then convert the load transfer function along the downwards direction in the self-balanced method into upwards direction. From that, the overall load-settlement curve of piles can be obtained with the actual measurements of the lower segments of piles as the boundary condition for the upper-segments of piles.

2 ANALYTICAL PREDICTION OF THE LOAD-DISPLACEMENT BEHAVIOR OF THE UPPER SEGMENT OF SELF-BALANCED PILES

2.1 Assumptions

Assuming the pile acting as a uniform cross-section linear elastic beam surrounded by single layer homogeneous soil, the equilibrium condition of the micro segment of the upper-segment of pile is shown in Fig.1. The relationship between axial force Q, self-weight G_u, perimeter u and side friction stress q_s is provided in the following equation.

$$\mathrm{d}Q(z)/\mathrm{d}z = -uq_s(W) - \gamma A \tag{1}$$

in which, q_s is function of the relative displacement between piles and soil (W), A is sectional area of pile, γ is the density of pile. Also with the assumption of pile acting as elastic bar, the following equation can be derived from the elastic stress-strain relationship of the pile.

$$-\mathrm{d}W/\mathrm{d}z = Q(z)/EA \tag{2}$$

From Equations (1) and (2), the basic relationship for the upper-segment of the pile is shown as the follows.

$$\mathrm{d}^2W/\mathrm{d}z^2 = uq_s(W)/EA + \gamma/E \tag{3}$$

In the above analytical descriptions, due to the different directions between the side frictions of piles in a self balanced pile test and in a static load test, the effects from self-weight of piles has been incorporated into the differential equations. The friction stress q_s along the pile can be described into load transfer function, a tri-linear model as shown in Fig. 2, which consists of an elastic state and two plastic hardening states. In this tri-linear model, λ_i is the shear modulus of the surrounding soil, S_{m1} is elastic displacement limit of the surrounding soil and S_{m2} is the displacement limit at the first plastic hardening.

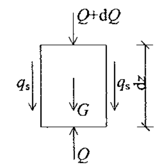

Fig. 1. Loading Diagram for the Micro Segment of Pile

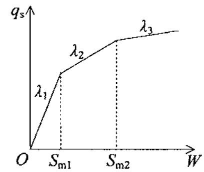

Fig. 2. Load Transfer Function between Pile and Surrounding Soil

2.2 Analytical Description for the Load-displacement Relationship of the Upper-segment of Pile

For the upper-segment of the pile, the surrounding soil is in elastic initially. With the load increased, plasticization happens in the soil near the loading cell and gradually develops upwards. After a certain load level, all surrounding soil becomes plastic in the second plastic hardening state. As shown in Fig.3, R_1, R_2, R_3 represent the height of regions of the three states, respectively. Substitute the load transfer function q_s into Equation (3), with consideration of the boundary condition at the top of pile (zero axial force) and the continuous conditions of surrounding soil in different states, the analytical description of load-displacement curve for the upper-segment of pile can be derived as follows.

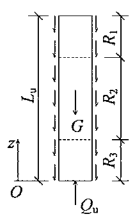

Fig. 3. Different Loading Stages for the Upper-Segment of Pile

as $\alpha_i = \sqrt{u\lambda_i / EA}$, $\beta_i = \alpha_i L_u$, $b_i = \alpha_i \,\mathrm{th}(\alpha_i R_i)$, ($i$=1,2,3), $m = (\alpha_1^2 - \alpha_2^2)/\alpha_2^2$, $G_u = \gamma A L_u$.

(i) All the soil surrounding the upper segment of pile keeps elastic. R_1=L_u.

$$Q_u = \alpha_1 EA \,\mathrm{th}\, \beta_1 (S_u + \gamma / E\alpha_1^2) \tag{4}$$

(ii) Part of the soil surrounding becomes plastic as the first plastic hardening state. R_1+ R_2=L_u.

$$\left.\begin{aligned} S_u &= (S_{m1} + \frac{\gamma}{E\alpha_1^2}) \frac{\alpha_1^2 \,\mathrm{ch}(\alpha_2 R_2) + \alpha_2 b_1 \,\mathrm{sh}(\alpha_2 R_2)}{\alpha_2^2} - mS_{m1} - \frac{\gamma}{E\alpha_2^2} \\ Q_u &= EA(mS_{m1} + S_u + \frac{\gamma}{E\alpha_2^2}) \frac{\alpha_1^2 b_2 + \alpha_2^2 b_1}{\alpha_1^2 + b_1 b_2} \end{aligned}\right\} \tag{5}$$

With the load increased, displacements of the surrounding soil have different behavior when

$$\frac{\alpha_1^2}{\alpha_2^2}(S_{m1} + \frac{\gamma}{E\alpha_1^2}) \,\mathrm{ch}\, \beta_2 > mS_{m1} + S_{m2} + \frac{\gamma}{E\alpha_2^2} \tag{6}$$

The soil reaches S_{m2} at the loading cell firstly, which means the beginning of the second plastic state. Otherwise, the soil reaches S_{m1} at the top of pile firstly, which means the end of the elastic state. If the surrounding soil at loading cell reaches the second hardening state firstly, with the load increased, the soil behaves as follow.
(iii) The three states exist simultaneously in the soil surrounding the upper segment of pile. $R_1+R_2+R_3=L_u$.

$$\left.\begin{aligned} S_u &= S_{m2}+(mS_{m1}+S_{m2}+\frac{\gamma}{E\alpha_2^2})[\frac{\alpha_2^2}{\alpha_3^2}\mathrm{ch}(\alpha_3 R_3)+\frac{\alpha_1^2 b_2+\alpha_2^2 b_1}{\alpha_1^2\alpha_3+\alpha_3 b_1 b_2}\mathrm{sh}(\alpha_3 R_3)-\frac{\alpha_2^2}{\alpha_3^2}] \\ Q_u &= EA(mS_{m1}+S_{m2}+\frac{\gamma}{E\alpha_2^2})[\frac{\alpha_2^2}{\alpha_3}\mathrm{sh}(\alpha_3 R_3)+\frac{\alpha_1^2 b_2+\alpha_2^2 b_1}{\alpha_1^2+b_1 b_2}\mathrm{ch}(\alpha_3 R_3)] \end{aligned}\right\} \tag{7}$$

As the continuous displacement at the boundary, equation (8) must be met.

$$(S_{m1}+\frac{\gamma}{E\alpha_1^2})\frac{\alpha_1^2\,\mathrm{ch}(\alpha_2 R_2)+\alpha_2 b_1\,\mathrm{sh}(\alpha_2 R_2)}{\alpha_2^2}=mS_{m1}+S_{m2}+\frac{\gamma}{E\alpha_2^2} \tag{8}$$

(iv) If the elastic region vanishes firstly, all the soil surrounding becomes plastic as the first plastic hardening state. $R_2=L_u$. And the equations in (iii) should be replaced by equation (9).

$$Q_u=\alpha_2 EA\,\mathrm{th}\,\beta_2(S_u+mS_{m1}+\gamma/E\alpha_2^2) \tag{9}$$

With the load increased, the soil behaves as mentioned.
(v) Part of the soil becomes plastic as the first plastic hardening state while others as the second plastic hardening state. $R_2+R_3=L_u$.

$$\left.\begin{aligned} S_u &= S_{m2}+(mS_{m1}+S_{m2}+\frac{\gamma}{E\alpha_2^2})[\frac{\alpha_2^2}{\alpha_3^2}\mathrm{ch}(\alpha_3 R_3)+\frac{b_2}{\alpha_3}\mathrm{sh}(\alpha_3 R_3)-\frac{\alpha_2^2}{\alpha_3^2}] \\ Q_u &= EA(mS_{m1}+S_{m2}+\frac{\gamma}{E\alpha_2^2})[\frac{\alpha_2^2}{\alpha_3}\mathrm{sh}(\alpha_3 R_3)+b_2\,\mathrm{ch}(\alpha_3 R_3)] \end{aligned}\right\} \tag{10}$$

(vi) All the soil surrounding becomes plastic as the second hardening state. $R_3=L_u$.

$$Q_u=\alpha_3 EA\,\mathrm{th}\,\beta_3[S_u-S_{m2}+\frac{\alpha_2^2}{\alpha_3^2}(mS_{m1}+S_{m2}+\frac{\gamma}{E\alpha_2^2})] \tag{11}$$

If $\lambda_3=0$, the second plastic hardening state becomes perfect plastic, and the equations relevant can be obtained using L Hospital rule. If $\lambda_3<0$, the first plastic hardening state becomes a softening state, and Euler's formula can be used to obtain relevant equations. As mentioned above, this tri-linear load transfer function can simulate different type of pile side resistance.

Through the analytical predictions of load-displacement for the upper segment of pile, the tri-linear load transfer function can be derived using the experimental measurements. As described in Fig. 1, the acting direction of the friction force for self-balanced piles is downwards. There is a need to verify certain parameters to convert the load transfer function to be suitable for the top-loading condition. According to Gong's paper in 2002, it can be achieved by dividing the parameters by coefficient η. For multi-layer soil, the coefficient η is calculated using the following equation.

$$\eta=L_u/\sum(L_i/\eta_i) \tag{12}$$

where L_i is the thickness of the i[th] layer, η_i is the correction coefficient of the i[th] layer. For clay and silt, η=0.8. For sand, η=0.7 and for rock, η=1.0.

3 ANALYTICAL METHOD TO CONVERT PREDICTION OF SELF-BALANCED PILES INTO LOAD-DISPLACEMENT CURVES FOR STATIC LOAD TEST PILES

3.1 Transforming Mechanism

The self-balanced pile is divided to upper and lower segments at the loading cell. Pile top load of the lower segment of pile is in equilibrium with the side friction resistance and the tip resistance of pile. The reaction force at the bottom of the upper segment of the pile is equal to the negative side friction resistance and self-weight of the pile. Therefore, the converting mechanism can be simplified into transforming the negative friction force along the upper segment of pile into the positive friction force of the static load pile. As shown in Fig.4, the loaded pile can be divided into two segments as shown in Fig.4 (b), in which the lower segment of the pile has the same transfer mechanism as the self-balanced piles. The Q_u-S_u curves of the self-balanced pile can be assumed as in accordance with that the axial loaded piles within the same region. With this assumption, the axial force and settlement caused by the top pressure and the positive side friction resistance of pile at the upper segment of pile can be calculated. As the boundary conditions, the top pressure and settlement of pile can be derived by solving the above differential equations with friction load transfer function being substituted in it.

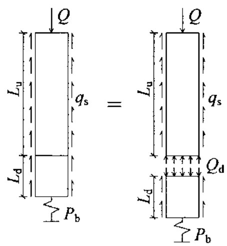

(a) (b)

Fig. 4. Loading Scheme of the Axial Loaded Pile

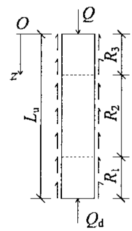

Fig. 5. Different Loading Stages for the the Upper-Segment of Axial Loaded Pile

3.2 Analytical Derivation of the Transforming Function

As shown in Fig.5, similar with section 2.1, assuming the pile acting as a uniform cross-section linear elastic bar with single-layer homogeneous soil around, the differential equation is shown as follows, without consideration of self-weight of piles (CHEN et al., 1994).

$$d^2W/dz^2 = uq_s(W)/EA \tag{13}$$

According to Equation (12), the transforming coefficient is re-evaluated, with corresponding updated values of parameters α_i, β_i, m. With substitution of each measurement of (Q_d, S_d) as boundary conditions, the state of the surrounding soil can be determined according to the relationship between S_d and S_{m1} or S_{m2}. The following section describes different situations, from which the (Q, S) relationship at the top of pile can be calculated according to each (Q_d, S_d) and finally obtain the load-settlement curves at the top of pile.

(1) $S_d \leq S_{m1}$

It means that the soil surrounding upper segment of pile is elastic at the location of the loading cell. Three conditions can be further considered according to the possible states of soil.

as $C_1 = \alpha_1 S_d \,\mathrm{sh}(\alpha_1 R_1) + \frac{Q_d}{EA}\mathrm{ch}(\alpha_1 R_1)$, $C_2 = \frac{\alpha_1^2}{\alpha_2} S_{m1}\,\mathrm{sh}(\alpha_2 R_2) + C_1\,\mathrm{ch}(\alpha_2 R_2)$,

$C_3 = \alpha_2 (S_d + mS_{m1})\mathrm{sh}(\alpha_2 R_2) + \frac{Q_d}{EA}\mathrm{ch}(\alpha_2 R_2)$

(i) All the soil surrounding the upper segment of pile keeps in elastic. $R_1=L_u$, requires $S \le S_{m1}$

$$\left.\begin{aligned} S &= S_d\,\mathrm{ch}\,\beta_1 + \frac{Q_d}{\alpha_1 EA}\mathrm{sh}\,\beta_1 \\ Q &= \alpha_1 EAS_d\,\mathrm{sh}\,\beta_1 + Q_d\,\mathrm{ch}\,\beta_1 \end{aligned}\right\} \tag{14}$$

(ii) Part of the soil surrounding the upper segment of pile becomes plastic as the first plastic hardening state. $R_1+R_2=L_u$, requires $S_{m1} \le S \le S_{m2}$

$$\left.\begin{aligned} S &= \frac{\alpha_1^2}{\alpha_2^2} S_{m1}\,\mathrm{ch}(\alpha_2 R_2) + \frac{C_1}{\alpha_2}\mathrm{sh}(\alpha_2 R_2) - mS_{m1} \\ Q &= \frac{\alpha_1^2}{\alpha_2} EAS_{m1}\,\mathrm{sh}(\alpha_2 R_2) + C_1 EA\,\mathrm{ch}(\alpha_2 R_2) \end{aligned}\right\} \tag{15}$$

From $S_d\,\mathrm{ch}(\alpha_1 R_1) + \frac{Q_d}{\alpha_1 EA}\mathrm{sh}(\alpha_1 R_1) = S_{m1}$ to determine R_1.

(iii) The three states exist simultaneously in the soil. $R_1+R_2+R_3=L_u$, requires $S > S_{m2}$

$$\left.\begin{aligned} S &= S_{m2} + \frac{\alpha_2^2}{\alpha_3^2}(mS_{m1} + S_{m2})[\mathrm{ch}(\alpha_3 R_3) - 1] + \frac{C_2}{\alpha_3}\mathrm{sh}(\alpha_3 R_3) \\ Q &= \frac{\alpha_2^2}{\alpha_3} EA(mS_{m1} + S_{m2})\mathrm{sh}(\alpha_3 R_3) + C_2 EA\,\mathrm{ch}(\alpha_3 R_3) \end{aligned}\right\} \tag{16}$$

R_1 can be determined from $S_d\,\mathrm{ch}(\alpha_1 R_1) + \frac{Q_d}{\alpha_1 EA}\mathrm{sh}(\alpha_1 R_1) = S_{m1}$,

and R_2 can be determined from $\frac{\alpha_1^2}{\alpha_2^2} S_{m1}\,\mathrm{ch}(\alpha_2 R_2) + \frac{C_1}{\alpha_2}\mathrm{sh}(\alpha_2 R_2) = mS_{m1} + S_{m2}$.

(2) $S_{m1} \le S_d \le S_{m2}$

It means that the soil surrounding the upper segment of pile becomes plastic as first plastic hardening state at the location of loading cell, which can be categorized into the following two conditions.

(i) All the soil surrounding the upper segment of pile becomes plastic as the first plastic hardening state. $R_2= L_u$, requires $S_{m1} \le S \le S_{m2}$

$$\left.\begin{aligned} S &= (S_d + mS_{m1})\,\mathrm{ch}\,\beta_2 + \frac{Q_d}{\alpha_2 EA}\mathrm{sh}\,\beta_2 - mS_{m1} \\ Q &= \alpha_2 EA(S_d + mS_{m1})\,\mathrm{sh}\,\beta_2 + Q_d\,\mathrm{ch}\,\beta_2 \end{aligned}\right\} \tag{17}$$

(ii) Part of the soil surrounding the upper segment of pile becomes plastic as the first plastic hardening state while others as the second plastic hardening state. $R_2+R_3=L_u$, requires $S > S_{m2}$

$$\left.\begin{aligned} S &= S_{m2} + \frac{\alpha_2^2}{\alpha_3^2}(mS_{m1} + S_{m2})[\mathrm{ch}(\alpha_3 R_3) - 1] + \frac{C_3}{\alpha_3}\mathrm{sh}(\alpha_3 R_3) \\ Q &= \frac{\alpha_2^2}{\alpha_3} EA(mS_{m1} + S_{m2})\mathrm{sh}(\alpha_3 R_3) + C_3 EA\,\mathrm{ch}(\alpha_3 R_3) \end{aligned}\right\} \tag{18}$$

R_2 can be determined from $(S_d + mS_{m1})\mathrm{ch}(\alpha_2 R_2) + \frac{Q_d}{\alpha_2 EA}\mathrm{sh}(\alpha_2 R_2) = mS_{m1} + S_{m2}$.

(3) $S_d \ge S_{m2}$

It means that all the soil surrounding the upper segment of pile becomes plastic as the second plastic hardening state and requires $S>S_{m2}$

$$\left.\begin{aligned} S &= S_{m2} - \frac{\alpha_2^2}{\alpha_3^2}(mS_{m1}+S_{m2}) + [\frac{\alpha_2^2}{\alpha_3^2}(mS_{m1}+S_{m2}) - S_{m2} + S_d]\operatorname{ch}\beta_3 + \frac{Q_d}{\alpha_3 EA}\operatorname{sh}\beta_3 \\ Q &= \alpha_3 EA[\frac{\alpha_2^2}{\alpha_3^2}(mS_{m1}+S_{m2}) - S_{m2} + S_d]\operatorname{sh}\beta_3 + Q_d\operatorname{ch}\beta_3 \end{aligned}\right\} \tag{19}$$

4 ENGINEERING CASE STUDY

Red Mountain Manor Project

Detailed experimental data for this project has been provided in the study by LIU et al. (1999). Cast-in-place bored piles have been used, with experimental measurements from both self-balanced method and heaped loading method. Detailed description of soil is listed in Table 1. The diameter of pile is 0.6 m with concrete grade of C25. Length of self-balanced pile is 25 m with loading cell located 9 m from the bottom of the pile. The self-weight of the upper segment of pile is 100kN with elastic modulus of pile 2.8×10^4 MPa. For the heaped loaded pile, the length of pile is 28m. According to the approach as described above, the parameters can be calculated as λ_1=11837 kPa/m, λ_2=3037 kPa/m, λ_3=1081 kPa/m, S_{m1}=0.98 mm, S_{m2}=5.54 mm. The load-displacement curves for the upper segment of pile are presented in Fig.6. With transforming coefficient of friction force as 0.65, 0.7 and 0.8, the measurements from self-balanced piles have been converted into load-displacement curves for axial loaded piles, which are compared with experimental measurements as shown in Fig.7.

Table 1. List of Parameters for Different Layer of Soil

Layer	Item	Depth (m)	Density (kN/m^3)	Porosity E	Liquidity Limit I_L	Shear Parameters c(kPa)	Shear Parameters φ(°)
①-2	Plain Fill	0~3.7	19.7	0.76	0.37	32.3	16.3
②-1	Clay		17.2	1.38	0.75	20.4	11.0
②-2	Silty Clay	2.2~15.0	18.7	0.97	1.09	14.4	21.0
②-3	Silty Clay		19.5	0.79	0.91	16.4	26.2
③	Silty Clay	16.0~27.0	19.8	0.74	0.37	51.0	19.7
④	Pebble soil with coarse sand	20.2~31.0	-	-	-	-	-

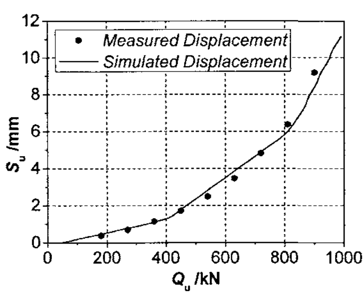

Fig. 6. Q_u-S_u Curves from Self-Balanced Piles

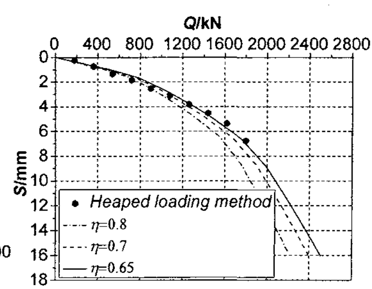

Fig. 7. Comparisons between Transforming Results with Experimental Measurements for Axial Loaded Piles

5 CONCLUSIONS

A load transfer method has been described in this paper with the assumption of the tri-linear load transfer function. The analytical expression of the load-displacement relationship for the upper segment of pile can be derived firstly with consideration of the deadweight of pile. Then, use the measured data of the lower segment of pile as the boundary condition, the results of self-balanced pile tests can be successfully converted into conventional load-settlement curve for static pile tests. The case study validated that the conventional pile load-settlement curve obtained by using this analytical method fit the measured data well. The tri-linear load transfer function is properly used to simulate various kinds of pile-soil interaction such as softening and perfect plasticity.

6 ACKNOWLEDGEMENTS

The work presented here is supported by the National Natural Science Foundation of China with the granted number 50779034. The authors wish to express their gratitude for the financial assistance. The anonymous reviewers' comments are also greatly acknowledged.

REFERENCES

Osterberg, J. (1989). New Device for load testing driven piles and drilled shaft separates friction and end bearing. *Piling and Deep Foundations*. pp. 421-427

Gong, W., et al. (2002). Theory and practice of self-balanced loading test for pile bearing capacity. *Journal of Building Structure*, 23(1), pp. 82-88.

Jiang, Y., et al. (2006). Analytical equation of loading-settlement curve under O-cell pile testing method. *Chinese Journal of Rock Mechanics and Engineering*, 25(S1), pp. 3258-3264.

Seed, H. B., and Reese L. C. (1957). The action of soft clay along friction piles. *Transactions, ASCE*, 122, pp. 731-754.

Chen, Z., and Hong, Y. (1995). Settlement Calculation of Single Pile and Piles Group, from Manual of Pile Foundation Engineering. *Beijing: China Architecture and Building Press*, pp.140-144.

Chen, L., et al. (1994). Analytical calculation of axial loading-settlement curve of piles. *Chinese Journal of Geotechnical Engineering*, 16(6), pp.30-38.

Liu, J., et al. (1999). The application of two-directional loading test on drilled shafts. *China Journal of Industrial Construction*, 29(3), pp.70-72.

Dai, G., et al. (2001). Engineering applications of a new static load testing method for piles with large bearing capacity in bridge. *Journal of Southeast University*, 31(4), pp.54-57.

Drilled Shaft Response in Piedmont Residuum Using Elastic Continuum Analysis and Seismic Piezocone Tests

Paul W. Mayne[1], M. ASCE, Fawad Niazi[2], and David Woeller[3]

[1]Professor, Geosystems Engineering Group, Civil & Environmental Engineering, Georgia Institute of Technology, Atlanta, GA 30332-0355 USA; paul.mayne@gatech.edu
[2]Graduate Research Assistant, Geosystems Engineering Group, Civil & Environmental Engineering, Georgia Institute of Technology, Atlanta, GA 30332-0355 USA: fniazi6@gatech.edu
[3]President, ConeTec Investigations Ltd., 2140 Vulcan Way, Richmond, British Columbia V6V 1J8 Canada; insitu@conetec.com

ABSTRACT: The axial load-displacement-capacity response of drilled shaft and bored pile foundations can be evaluated during the analysis and design stage using an elastic continuum framework and results from in-situ testing methods, in particular, the seismic piezocone test (SCPTù). The SCPTù is an optimal and economical means for collection of geotechnical data because the same sounding provides up to five separate measurements with depth: cone tip resistance (q_t), sleeve friction (f_s), porewater pressure (u_2), time rate of consolidation (t_{50}), and shear wave velocity (V_s). Moreover, the SCPTù provides information on soil behavior at both ends of the stress-strain-strength curves, namely the peak strength and geostatic stress state for evaluating axial pile capacity and the small-strain stiffness ($G_{max} = \rho_t \cdot V_s^2$) for the initial soil-pile deformations. Using a Randolph-type analytical elastic pile model, the approach can handle either traditional top down compression loading by dead-weight or reaction beam systems, or the more recent Osterberg cell that juxtaposes base and side resistances in opposite directions. A case study involving O-cell tests on a drilled shaft in Piedmont residuum and partially-weathered rock in Atlanta are presented.

INTRODUCTION

The axial load-displacement response and load-transfer distribution of piles can be evaluated rationally within an elastic continuum solution (Poulos & Davis, 1980). Of particular convenience, the closed-form analytical solution of Randolph & Wroth (1978, 1979) can handle rigid piles, compressible piles, and very long piles, as well as presence of a lower stiffer soil or rock layer, homogeneous or Gibson soil modulus variations with depth, and straight or belled shafts (Fleming et al. 1992).

The Osterberg load cell (O-cell) is an innovative and convenient means for mobilizing both the axial side and base resistance components of drilled shaft foundations, also termed bored piles (Fellenius 2001). The O-cell is placed in the drilled shaft foundation during the installation of the rebar cage and then concreted in-place. During load testing, the hydraulic jack is inflated using a high-pressure pump, thereby lifting the one upper shaft section while simultaneously pushing the lower segment section downward (Osterberg 2000). The results are evaluated to obtain the mobilized side and base resistances, as well as derivation of an equivalent top-down curve for the axial load-displacement-capacity response of the bored pile.

In the original setup, the O-cell was positioned at the base of the bored pile, yet can be installed at any convenient elevation within the shaft. Multiple levels of O-cells can be installed to stage-load the bored pile in sections, thereby achieving huge capacities during load testing. The analysis of individual segments from O-cell tests, as well as top-down loading, is conveniently handled using the Randolph-Wroth analytical model, as depicted in Figure 1. For clarity, the solution here is presented for rigid pile segments, yet can be easily upgraded to account for pile compressibility effects and stiffer geomaterials under the base, if desired.

O-Cell Elastic Solution

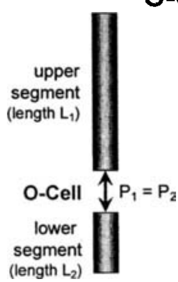

Rigid pile shaft under upward loading

$$\frac{P_1}{G_{s1} r_{o1} w_1} = \frac{2\pi}{\zeta_1} \cdot \frac{L_1}{r_{o1}}$$

Rigid pile under compression loading

$$\frac{P_2}{G_{s2} r_{o2} w_2} = \frac{4}{(1-\upsilon)\xi} + \frac{2\pi}{\zeta_2} \cdot \frac{L_2}{r_{o2}}$$

P = applied force
L = pile length
r_o = pile shaft radius
E_p = pile modulus
G_s = soil shear modulus along sides
ν = Poisson's ratio of soil

w = pile displacement
$\lambda = E_p/G_{sL}$ = soil-pile stiffness ratio
$\xi = G_{s2}/G_{sb}$ (Note: floating pile: $\xi = 1$)
G_{sb} = soil modulus below pile base/toe
$\zeta = \ln(r_m/r_o)$ = soil zone of influence
$r_m = L\{0.25 + \xi\,[2.5\,(1-\nu) - 0.25]\}$

Figure 1. Osterberg cell evaluation using elastic continuum solution.

DRILLED SHAFT CASE STUDY IN PIEDMONT RESIDUUM

A case study involving O-cell load testing of a drilled shaft for a Georgia DOT viaduct next to CNN in downtown Atlanta is used to illustrate the approach. The soil borings indicated residual silts and sands grading to saprolite and partially-weathered rock of the Piedmont geology, as shown in Figure 2. Very high blow-counts were recorded below depths of 11 m. The site was also explored by a GT crew using seismic piezocone penetration tests (SCPTù), as presented in Figure 3. Equivalent *N*-values from the CPT tip resistance (q_t) at the site were obtained from the CPT - SPT